Обзор ArXiv/astro-ph, 16-29 октября 2019 года

От Сильченко О.К.

ArXiv: 1910.06345

Stellar feedback sets the universal acceleration scale in galaxies

Michael Y. Grudić[1,3★], Michael Boylan-Kolchin[2], Claude-André Faucher-Giguère[1], and Philip F. Hopkins[3]

[1] *Department of Physics and Astronomy and CIERA, Northwestern University, 2145 Sheridan Road, Evanston, IL 60208, USA*
[2] *Department of Astronomy, The University of Texas at Austin, 2515 Speedway, Stop C1400, Austin, TX 78712, USA*
[3] *TAPIR, Mailcode 350-17, California Institute of Technology, Pasadena, CA 91125, USA*

Accepted XXX. Received YYY; in original form ZZZ

ABSTRACT

It has been established for decades that rotation curves deviate from the Newtonian gravity expectation given baryons alone below a characteristic acceleration scale $g_\dagger \sim 10^{-8}\,\mathrm{cm\,s^{-2}}$, a scale promoted to a new fundamental constant in MOND-type theories. In recent years, theoretical and observational studies have shown that the star formation efficiency (SFE) of dense gas scales with surface density, $\mathrm{SFE} \sim \Sigma/\Sigma_{\rm crit}$ with $\Sigma_{\rm crit} \sim (\dot{p}/m_*)/(\pi^2 G) \sim 1000\,\mathrm{M_\odot\,pc^{-2}}$ (where $\dot{p}/m_*$ is the momentum flux output by stellar feedback per unit stellar mass formed). We show that the star formation efficiency, more correctly, scales with the gravitational acceleration, i.e. that $\mathrm{SFE} \sim g_{\rm tot}/g_{\rm crit} \equiv (G\,M_{\rm enc}/R^2)/([\dot{p}/m_*]/\pi)$, where $M_{\rm enc}(<r)$ is the total gravitating mass and

Lelli et al. (2017): RAR!

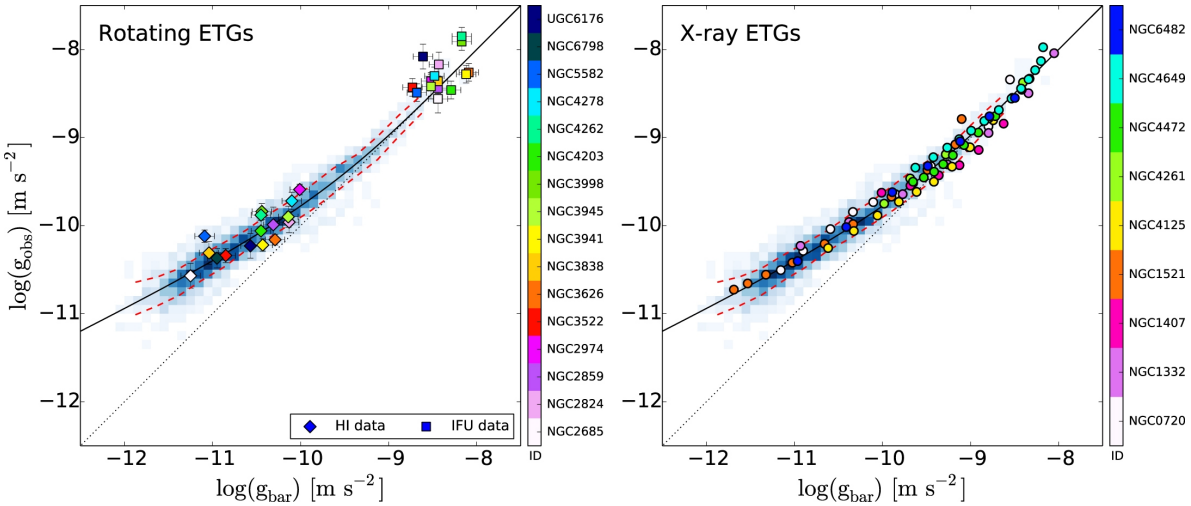

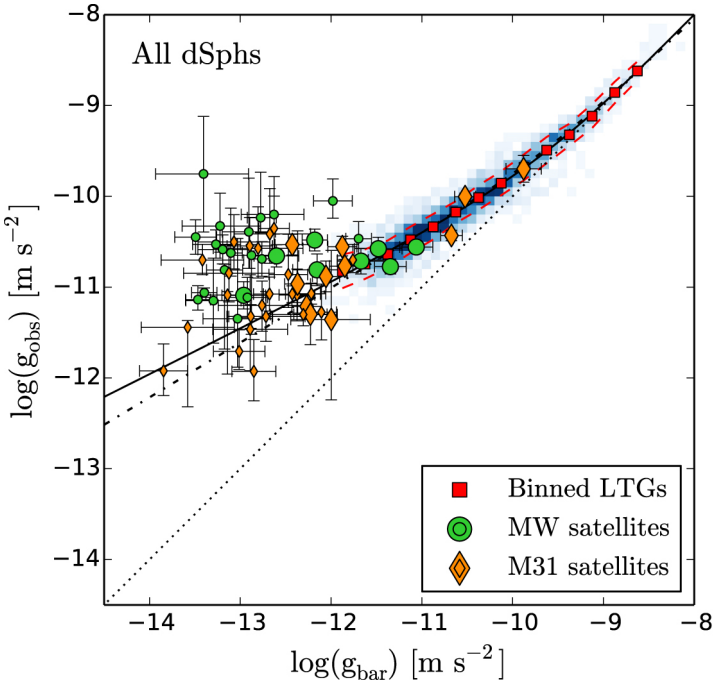

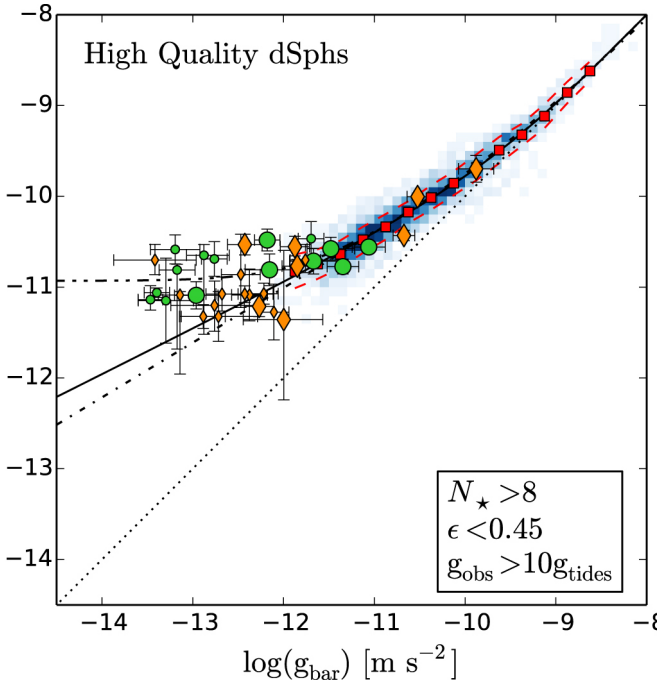

Формулы для feedback'a!

$$\frac{M_{*,\,\mathrm{young}}}{M_{\mathrm{gas,\,expelled}}} \sim \frac{\pi\, G\, M_{\mathrm{tot}}}{\langle \dot{p}/m_* \rangle\, R^2} = \frac{\Sigma_{\mathrm{tot}}}{\Sigma_{\mathrm{crit}}} \qquad (1)$$

where $\Sigma_{\mathrm{tot}} \equiv M_{\mathrm{tot}}/A$ and $\Sigma_{\mathrm{crit}} \equiv \langle \dot{p}/m_* \rangle/(\pi^2\, G)$.

In the last few years, a considerable body of work has explored the SFE and demonstrated that such a scaling, with a roughly constant $\Sigma_{\mathrm{crit}} \sim 1000\,\mathrm{M}_\odot\,\mathrm{pc}^{-2}$, works remarkably well at describing both observations (e.g., Wong et al. 2019) and detailed numerical simulations of cloud collapse (e.g.,

gravitational acceleration from all matter, $g_{\mathrm{tot}} = G\, M_{\mathrm{tot}}/r^2$. Noting this, Eq. 1 can be rewritten as

$$\frac{M_{*,\,\mathrm{young}}}{M_{\mathrm{gas,\,expelled}}} \sim \frac{\pi\, G\, M_{\mathrm{tot}}}{\langle \dot{p}/m_* \rangle\, R^2} = \frac{g_{\mathrm{tot}}}{g_{\mathrm{crit}}} \qquad (2)$$

$$g_{\mathrm{crit}} \equiv \frac{1}{\pi}\,\langle \dot{p}/m_* \rangle = \pi\, G\, \Sigma_{\mathrm{crit}} \sim 2 \times 10^{-8}\,\mathrm{cm\,s}^{-2} \sim \mathrm{g}_\dagger.$$

Expressed in cgs units, we see that $g_{\mathrm{crit}} \sim 0.3\,\langle \dot{p}/m_* \rangle$ corresponds numerically to the "universal" acceleration $g_\dagger$ of galaxies.

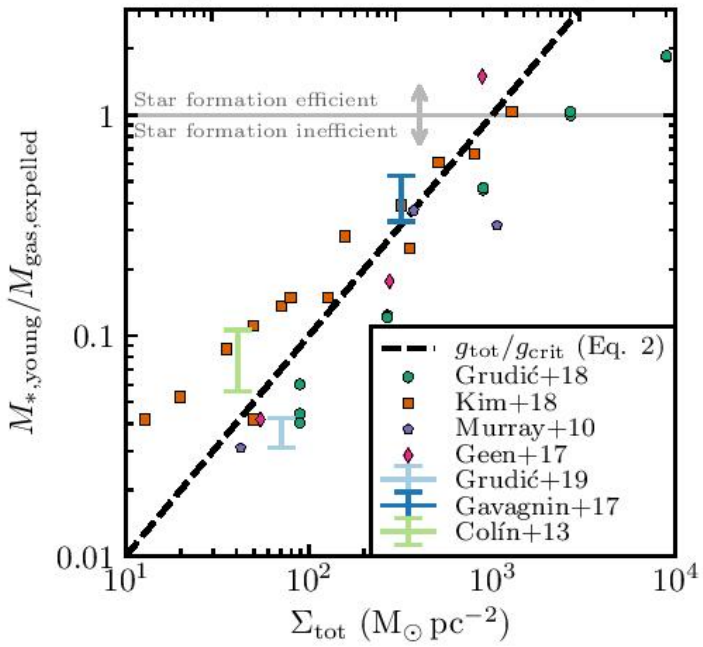

Figure 1. Ratio of the young stellar mass formed to the expelled gas mass in GMCs predicted by different theoretical models as a function of total mass surface density Σ_{tot}, which is equivalent to an effective acceleration $g_{\mathrm{tot}} \equiv \pi G \Sigma_{\mathrm{tot}}$, plotted on top in units of $g_\dagger$ (the observed characteristic acceleration scale of galaxies).

И вот какая физика предлагается для RAR

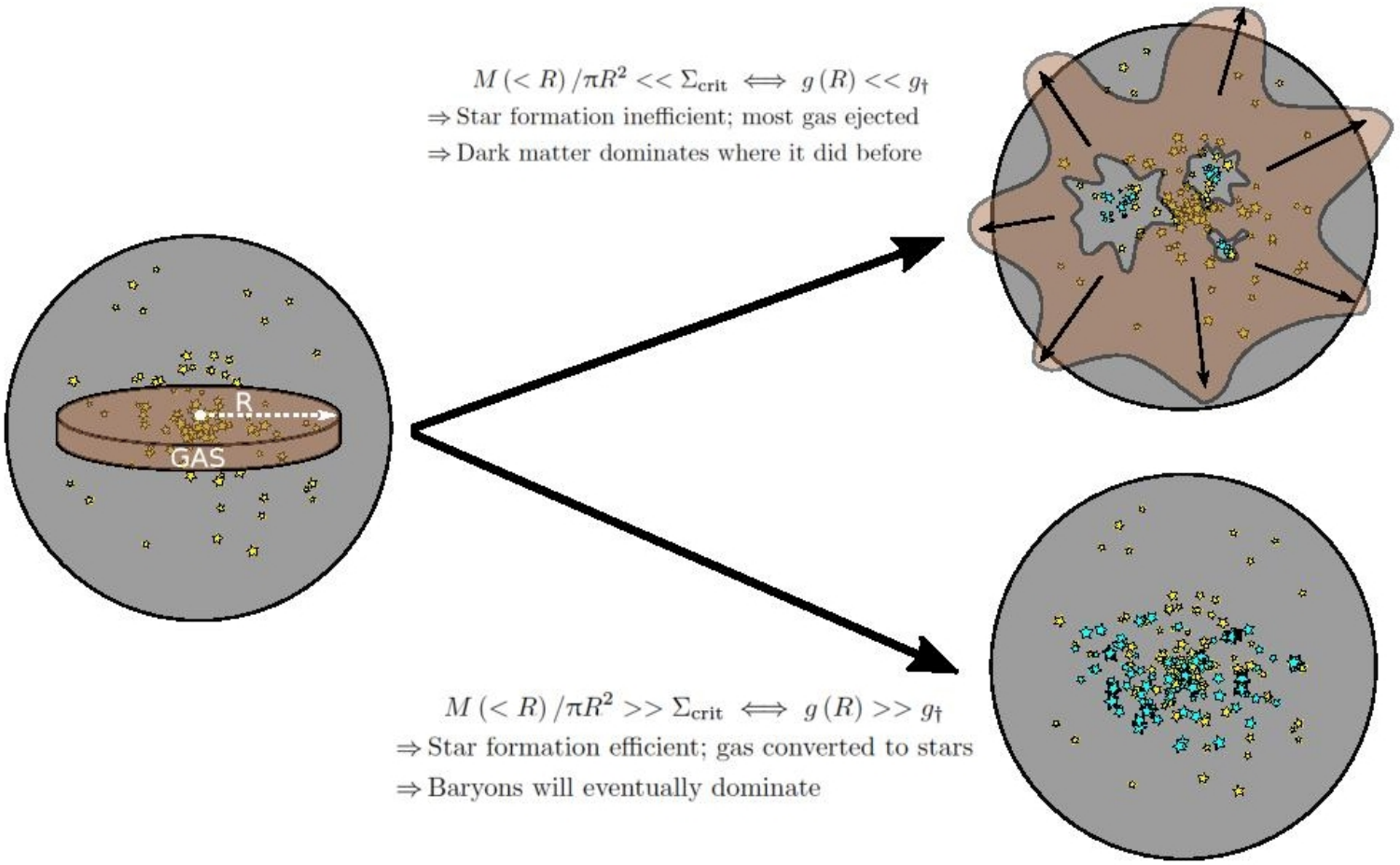

И это универсальное ускорение выражается через фундаментальные постоянные!

2.4 Expressing $g_\dagger$ in Fundamental Constants

According to the picture proposed here, $g_\dagger \sim g_{\rm crit} \sim 0.3\,\langle \dot{p}/m_* \rangle$. But $\langle \dot{p}/m_* \rangle$ itself can be understood in terms of the stellar IMF and the physics of massive stars. As discussed in §2.1, the stellar population-averaged $\dot{p} \sim L/c$ (i.e. $\langle \dot{p}/m_* \rangle \sim c^{-1}\,(L/M)_{*,\,\rm young}$) for a variety of feedback mechanisms, and the most massive stars dominate the luminosity and feedback. The luminosities of these stars are set by the Eddington limit:

$$L_{\rm Edd,\,i} = \frac{4\pi G m_{\rm p} c}{\sigma_{\rm T}} M_i, \tag{6}$$

where M_i is the mass of an individual massive star and $\sigma_{\rm T}$ is the Thomson cross-section. So $(L/M)_{*,\,\rm young} \sim f_{\rm massive}\,L_{\rm Edd,\,i}/M_i$ where the $f_{\rm massive}$ is the mass fraction in massive stars: to reproduce the more accurate full stellar population calculation for a standard IMF (Leitherer et al. 1999), $f_{\rm massive} \sim 0.03$.[5] Thus we have $\langle \dot{p}/m_* \rangle \sim f_{\rm massive}\,(4\pi\,G\,m_{\rm p})/\sigma_{\rm T}$. Putting these together, we obtain:

$$g_\dagger \sim g_{\rm crit} \sim (4\,f_{\rm massive})\,\frac{G m_{\rm p}}{\sigma_{\rm T}} \sim 0.1\,\frac{G m_{\rm p}}{\sigma_{\rm T}} \sim 0.5\,G m_{\rm p}\left(\frac{m_{\rm e} c}{\alpha \hbar}\right)^2, \tag{7}$$

where the last expression uses $\sigma_{\rm T} \equiv \frac{8\pi}{3}\left(\frac{\alpha \hbar c}{m_{\rm e} c^2}\right)^2$, in terms of the fine-structure constant α, the Planck constant $\hbar = h/2\pi$, the electron mass m_e, and the speed of light c.

ArXiv: 1910.06984

HALF-MASS RADII OF QUIESCENT AND STAR-FORMING GALAXIES EVOLVE SLOWLY FROM $0 \lesssim z \leq 2.5$: IMPLICATIONS FOR GALAXY ASSEMBLY HISTORIES*

KATHERINE A. SUESS[1], MARISKA KRIEK[1], SEDONA H. PRICE[2], GUILLERMO BARRO[3]

Draft version October 17, 2019

ABSTRACT

We use high-resolution, multi-band imaging of ∼16,500 galaxies in the CANDELS fields at $0 \lesssim z \leq 2.5$ to study the evolution of color gradients and half-mass radii over cosmic time. We find that galaxy color gradients at fixed mass evolve rapidly between $z \sim 2.5$ and $z \sim 1$, but remain roughly constant below $z \sim 1$. This result implies that the sizes of both star-forming and quiescent galaxies increase much more slowly than previous studies found using half-light radii. The half-mass radius evolution of quiescent galaxies is fully consistent with a model which uses observed minor merger rates to predict the increase in sizes due to the accretion of small galaxies. Progenitor bias may still contribute to the growth of quiescent galaxies, particularly if we assume a slower timescale for the minor merger growth model. The slower half-mass radius evolution of star-forming galaxies is in tension with cosmological simulations and semi-analytic galaxy models. Further detailed, consistent comparisons with simulations are required to place these results in context.

Subject headings: galaxies: evolution — galaxies: formation — galaxies: structure

Выборка – больше 10000 галактик

2. SAMPLE, METHODS, & GALAXY HALF-MASS RADII

In this Letter, we present the evolution of galaxy half-mass radii from $z = 2.5$ to $z \sim 0$. From $1.0 \leq z \leq 2.5$, we use the sample of galaxy half-mass radii presented in Suess et al. (2019). This high-redshift sample consists of 7,006 galaxies selected from the ZFOURGE photometric

Here, we expand our previous work by presenting the half-mass radii of an additional 9,543 galaxies at $z \leq 1.0$. This low-redshift sample consists of all galaxies in the 3D-HST photometric catalog with $z \leq 1.0$, $\log M_*/M_\odot > 9.0$, $\mathrm{S/N_{F160W}} \geq 10$, a use flag equal to one, and a convergent GALFIT fit. These selection criteria are equivalent to those of the higher-redshift sample presented in Suess et al. (2019), but using the 3D-HST catalogs as opposed to the ZFOURGE catalogs. This allows us to include galaxies from the AEGIS and GOODS-N fields (not included in ZFOURGE) and better sample the $z \lesssim 0.5$ universe. Furthermore, we note that recovered galaxy properties at $z < 1$ do not change significantly with the inclusion of the ZFOURGE data: at these low redshifts, the medium-band filters in ZFOURGE no longer sample the Balmer break.

Если перейти от радиуса по светимости к радиусу по массе…

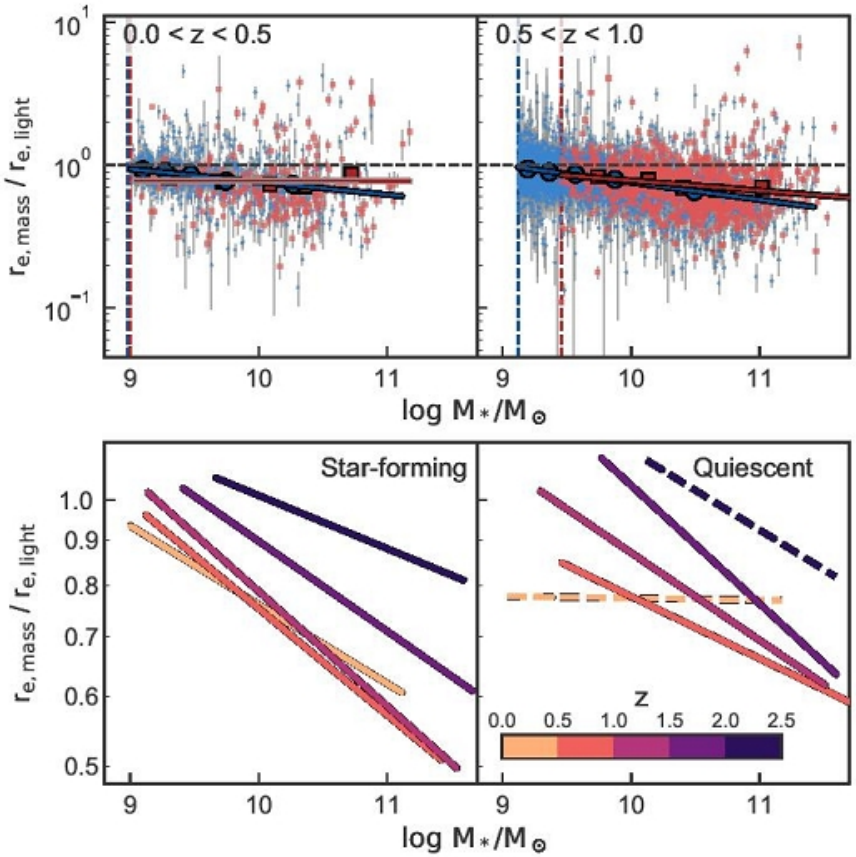

FIG. 1.— Top: color gradient strength as a function of stellar mass for two redshift intervals. Small light blue points and light red squares show individual star-forming and quiescent galaxies; large blue points and red squares show a running median. The blue and red lines show best-fit linear relations to each trend; lines are outlined in black if the slope of the relation is inconsistent with zero, and outlined in grey if the slope is consistent with zero. Dashed vertical blue and red lines show the mass completeness of the star-forming and quiescent samples. Bottom: best-fit relation between color gradient strength and stellar mass for star-forming (left) and quiescent (right) galaxies as a function of redshift. Dashed lines represent fits whose slopes are consistent with zero. We see clear redshift evolution in the best-fit color gradient-mass relations for both quiescent and star-forming galaxies.

То за счет градиента цвета эволюция радиуса уменьшится в разы

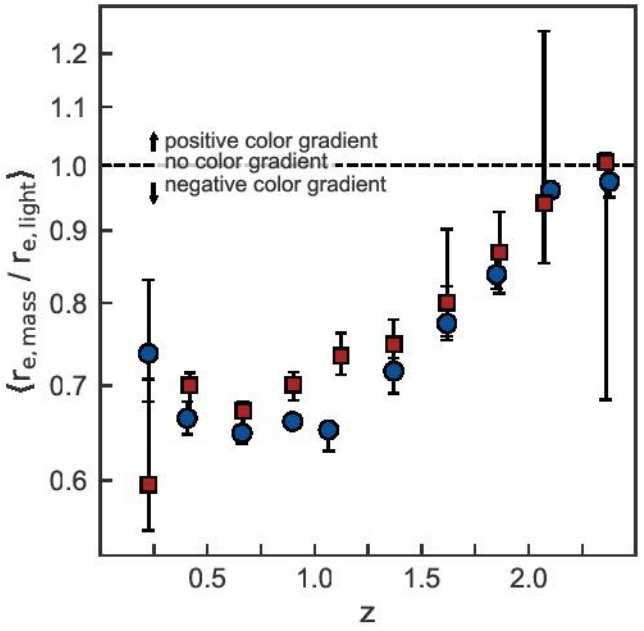

FIG. 2.— Median half-mass to half-light radius ratio for star-forming and quiescent galaxies (blue circles and red squares) as a function of redshift. $r_{\rm mass}/r_{\rm light}$ traces the strength of radial color gradients; values less than one indicate negative color gradients, where the center of the galaxy is redder than the outskirts. Only galaxies with $\log M_*/M_\odot > 10.1$, where our sample is complete, are included. Error bars show the central 68% of 500 bootstrap

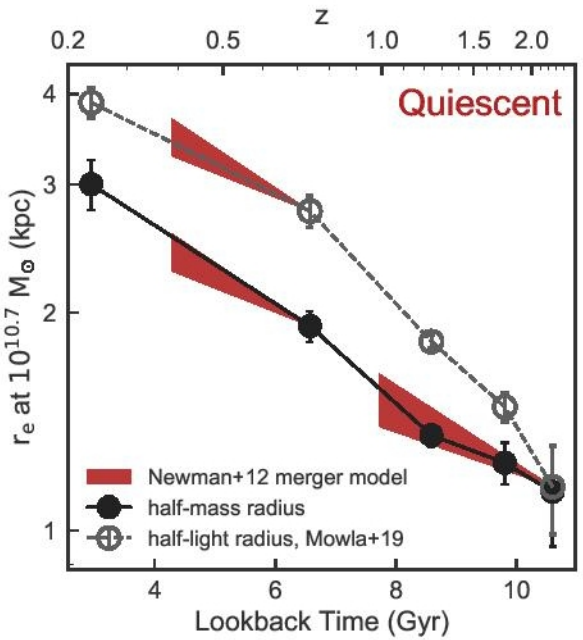

FIG. 3.— Half-light radius (open grey points) and half-mass radius (filled black points) of quiescent galaxies at $10^{10.7} M_\odot$ as a function of lookback time. Red shaded regions show the expected growth via minor mergers using the Newman et al. (2012) models, assuming a merger timescale of $\tau_e = 1.0$ Gyr. Minor mergers alone are sufficient to explain the growth of half-mass radii.

Но все-таки согласуется с minor merging!

ArXiv: 1910.10446

Disk Growth and Quenching

Ying-jie Peng[1,2⋆], and Alvio Renzini[3]†
[1]*Kavli Institute for Astronomy & Astrophysics, Peking University, 5 Yiheyuan Road, Beijing 100871, China*
[2]*Department of Astronomy, , School of Physics, Peking University, 5 Yiheyuan Road, Beijing 100871, China*
[3]*INAF - Osservatorio Astronomico di Padova, Vicolo dell'Osservatorio 5, I-35122 Padova, Italy*

Accepted October 23, 2019; Received August 21, 2019, in original form

ABSTRACT
Based on well established scaling relation for star forming galaxies as a function of redshift, we argue that the implied growth by a large factor of their angular momentum requires that the angular momentum of the inflowing gas fuelling star formation and disk growth must also secularly increase. We then propose that star formation in disks can cease (quench) once the accreted material (mainly atomic hydrogen) comes in with excessive angular momentum for sustaining an adequate radial flow of cold, molecular gas. Existing observational evidence supporting this scenario is mentioned, together with some future observational studies that may validate (or invalidate) it.

Перечисление, что и как меняется у дисковых галактик с z

well established *scaling relations*, here briefly recalled.

At fixed stellar mass, the half-light radius R_h of disks scales as $\sim (1+z)^{-1}$ (Newman et al. 2012; Mosleh et al. 2012; Shibuya et al. 2015; Lilly & Carollo 2016; Mowla et al. 2019), so it increases by roughly a factor of ~ 3 over the last ~ 10 Gyr. This becomes a lower limit if one follows the evolution of individual galaxies, as they growth also in mass and sizes increase with stellar mass, roughly as $R_h \sim M_*^{0.2}$ (van der Wel et al. 2014; Mowla et al. 2019). However, these figures refer to half-light radii, whereas half-mass radii appear to evolve slower, e.g., as $\sim (1+z)^{-0.5}$ (Mosleh et al. 2017), or even more so according to Suess et al. (2019). Measured half-mass radii are still affected by large errors and different measuring procedures can result in very large differences for individual sources, though the distribution of the half-mass to half-light radii shows a sharp peak at 1, i.e., the two radii being equal (Suess et al. 2019).

Disks at $z \sim 2$ have a much higher molecular gas fraction (~ 50 per cent) than nearby disks (Tacconi et al. 2010; Daddi et al. 2010; Genzel et al. 2015; Scoville et al. 2017), which to first order scales as $\sim (1+z)^{2.6}$ (Tacconi et al. 2018). Combining these two scaling relations we see that the surface gas density for fixed stellar mass scales as $\sim (1+z)^{4.6}$, which means that at $z \sim 2$ it is ~ 150 times (!) higher than in local disks of the same mass.

Likely as a result of higher molecular gas content and gas density, the star formation rate (SFR) at fixed stellar mass increases as $\sim (1+z)^{2.8}$ (e.g., Speagle et al. 2014; Ilbert et al. 2015). Indeed, the close similarity of the two exponents of the molecular gas fraction and SFR scaling relations (that could actually be identical when allowing for the errors) imply that a Schmidt-like relation has been in place at least over the last 10 Gyr, and with a exponent close to unity

Из этих НАБЛЮДАЕМЫХ зависимостей следует, что за 10 млрд лет в 30 раз вырос момент аккрецируемого газа

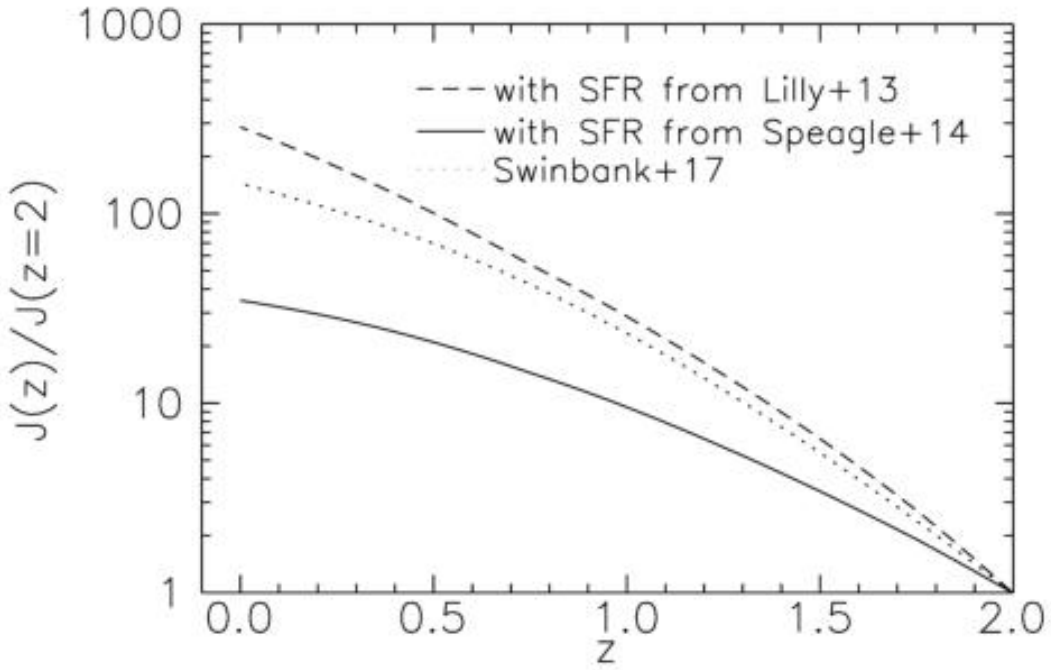

Figure 1. The average secular increase of the angular momentum of star-forming disks since $z = 2$ for two choices of the SFR(M_*, z) relation, from Lilly et al. (2013) and Speagle et al. (2014), as indicated. The angular momentum scaling from Swinbank et al. (2017) is also shown.

А это механизм quenching'a!

ArXiv: 1910.08794

Discovery of a large HI ring around the quiescent galaxy AGC 203001

Omkar Bait,[1]★, Sushma Kurapati[1], Pierre-Alain Duc[2], Jean-Charles Cuillandre[3], Yogesh Wadadekar[1], Peter Kamphuis[4] and Sudhanshu Barway[5]

[1] *National Centre for Radio Astrophysics, Tata Institute of Fundamental Research, Post Bag 3, Ganeshkhind, Pune 411007, India*
[2] *Universitè de Strasbourg, CNRS, Observatoire astronomique de Strasbourg, UMR 7550, F-67000 Strasbourg, France*
[3] *AIM, CEA, CNRS, Universitè Paris-Saclay, Universitè Paris Diderot, Sorbonne Paris Citè, Observatoire de Paris, PSL University, 91191 Gif-sur-Yvette Cedex, France*
[4] *Astronomisches Institut Ruhr-Universität Bochum (AIRUB), Universitätsstrasse 150, D-44780 Bochum, Germany*
[5] *Indian Institute of Astrophysics (IIA), II Block, Koramangala, Bengaluru 560 034, India*

Гигантское кольцо HI вокруг эллиптической галактики

Table 1. General properties of the HI ring.

Total detected HI flux	1.13 ± 0.13 Jy km/s
Systematic velocity	5602.54 km/s
Velocity width	28.52 km/s (W50), 99.80 km/s (W20)
Ellipticity	0.67
Position angle of the major-axis	20°
Peak column density	1.1×10^{20} cm^{-2}

4 THE HI RING AROUND AGC 203001

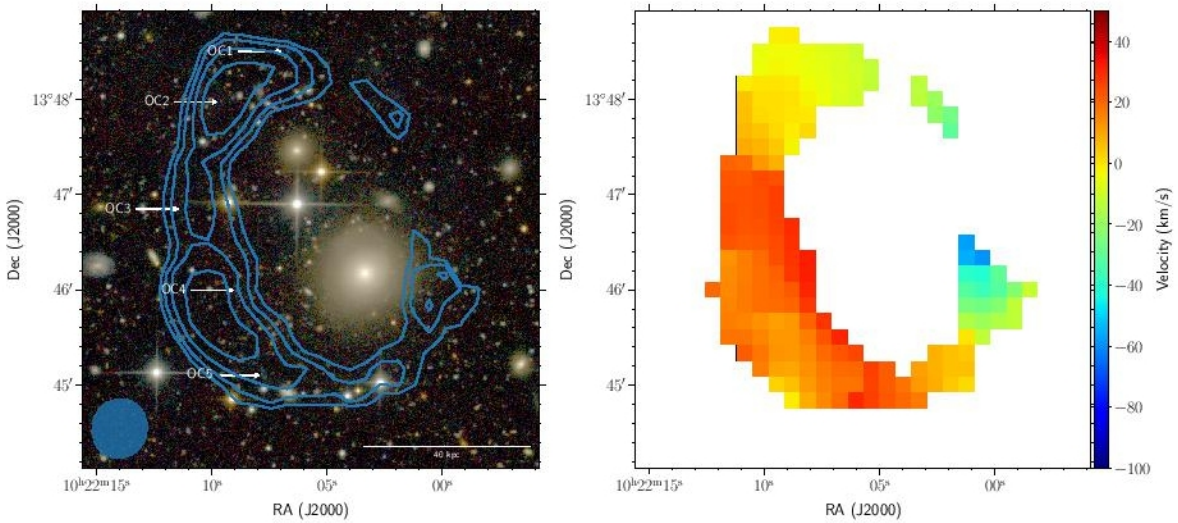

Figure 1. Left Panel: The HI ring around AGC 203001 in blue contours overlaid on the CFHT optical g, r, i-band color composite image. The lowest contour corresponds to a HI column density of 2.8×10^{19}cm^{-2} and subsequent contours rise in multiples of $\sqrt{2}$. The HI ring has a projected diameter of ∼ 115 kpc. The arrows show the positions of the identified optical counterparts. Right Panel: The HI velocity map of the ring.

Вообще-то, это группа – как LeoI

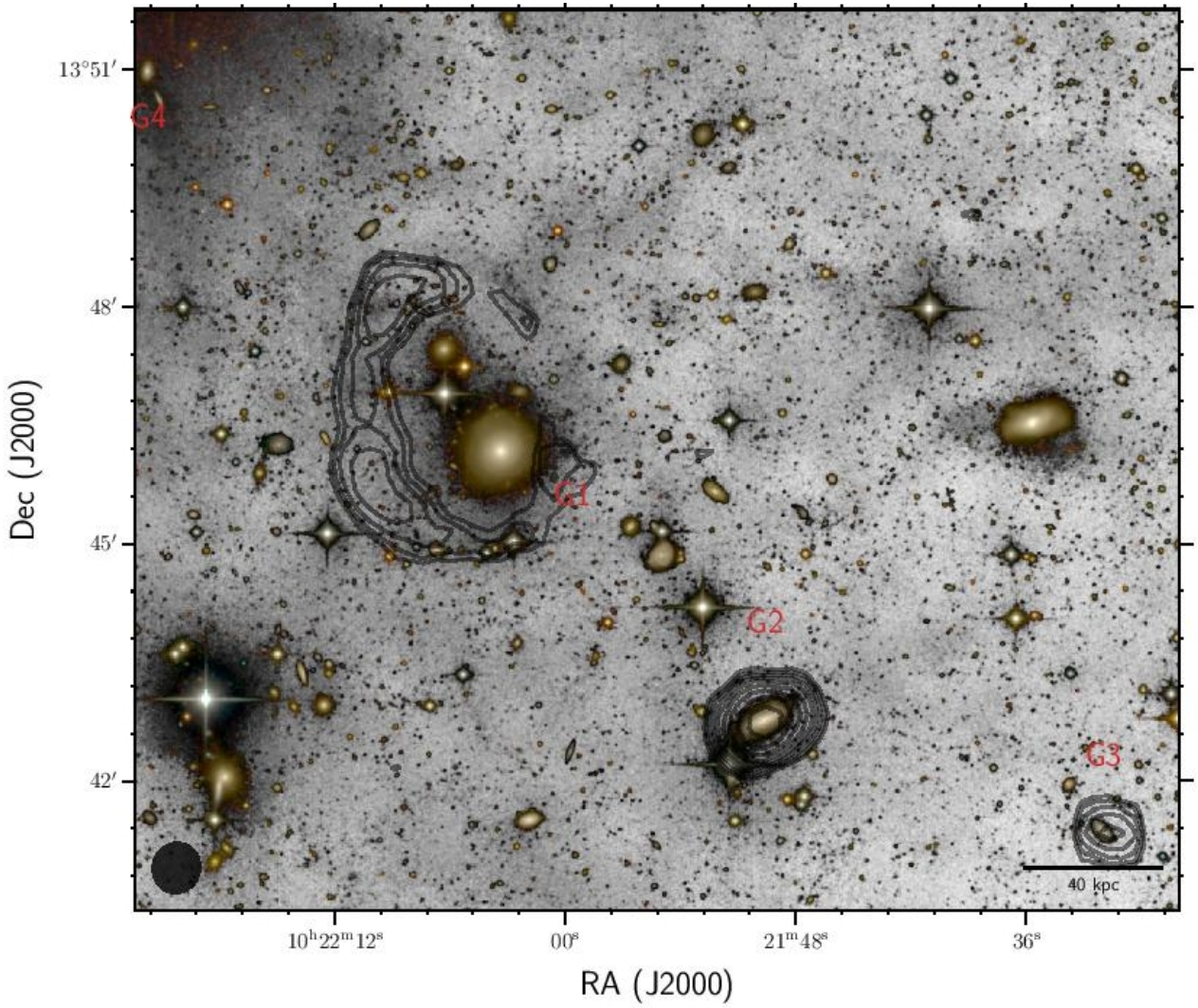

Figure 4. Large scale image of the HI ring overlaid on the CFHT g-band image shown in reversed greyscale wherein the background is

Это большая редкость?

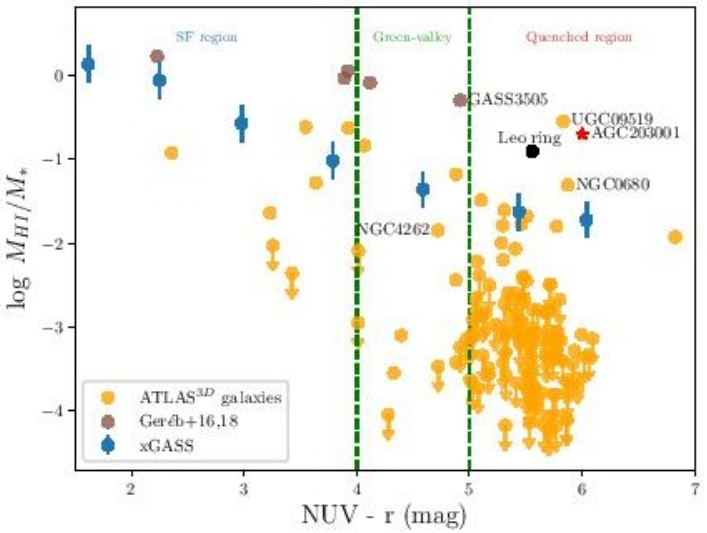

Figure 5. The HI gas fraction vs. $NUV-r$ plane. The blue points represent the median values from the xGASS survey (Catinella et al. 2018). AGC 203001 is marked with a red star and the Leo ring is marked with a black point. The yellow points represent the ATLAS^{3D} galaxies and the brown points represent the HI-excess galaxies (with GASS3505 highlighted) from (Geréb et al. 2016, 2018). The names of some of the HI-rich ATLAS^{3D} galaxies, UGC09519 and NGC0680, and a ring galaxy NGC4262 are highlighted. The region within the green dashed line correspond to the green-valley from Salim (2014), and the region on the left and right corresponds to the SF and quenched region respectively. See text for discussion.

ArXiv: 1910.10158

An Extremely Massive Quiescent Galaxy at $z = 3.493$: Evidence of Insufficiently Rapid Quenching Mechanisms in Theoretical Models*

Ben Forrest,[1] Marianna Annunziatella,[2] Gillian Wilson,[1] Danilo Marchesini,[2] Adam Muzzin,[3] M. C. Cooper,[4] Z. Cemile Marsan,[3] Ian McConachie,[1] Jeffrey C. C. Chan,[1] Percy Gomez,[5] Erin Kado-Fong ,[6] Francesco La Barbera,[7] Ivo Labbé,[8] Daniel Lange-Vagle,[2] Julie Nantais,[9] Mario Nonino,[10] Theodore Peña,[2] Paolo Saracco,[11] Mauro Stefanon,[12] and Remco F. J. van der Burg[13]

[1] *Department of Physics and Astronomy, University of California, Riverside, CA 92521, USA*
[2] *Physics Department, Tufts University, Medford, MA, USA*
[3] *Department of Physics and Astronomy, York University, Toronto, Ontario, Canada*
[4] *Center for Cosmology, Department of Physics and Astronomy, University of California, Irvine, Irvine, CA, USA*
[5] *W. M. Keck Observatory, Kamuela, HI, USA*
[6] *Department of Astrophysical Sciences, Princeton University, Princeton, NJ, USA*
[7] *INAF–Osservatorio Astronomico di Capodimonte, Napoli, Italy*
[8] *Centre for Astrophysics & Supercomputing, Swinburne University of Technology, Hawthorn, VIC, Australia*
[9] *Departamento de Ciencias Físicas, Universidad Andrés Bello, Santiago, Chile*
[10] *INAF–Osservatorio Astronomico di Trieste, Trieste, Italy*
[11] *INAF–Osservatorio Astronomico di Brera, Milano, Italy*
[12] *Leiden Observatory, Leiden University, Leiden, Netherlands*
[13] *European Southern Observatory, Garching, Germany*

Уникальная массивная галактика без SF, z=3.5

In this letter, we present deep rest-frame optical spectra of XMM-2599, a quiescent UMG candidate at $z_{\rm phot} \sim 3.4$. Our spectra confirm its quiescent nature and imply a period of intense star formation ($>$ 1000 $M_\odot$/yr) in its $z \sim 5.5$ progenitor, consistent with most DSFGs observed at that epoch. The spectroscopic confirmation of XMM-2599, the most massive quiescent galaxy at $z > 3$, arguably represents the biggest challenge yet to the latest theoretical models of galaxy formation in the early Universe, underlining the inadequate quenching mechanism(s) currently implemented in simulations.

from SED modeling). Taken together, these three characteristics strongly suggest this galaxy is observed when the Universe was only 1.5-2.0 billion years old, has a stellar mass $\log(M_*/M_\odot) \sim 11.5$, and is no longer forming stars at an appreciable rate. As shown in Figure 1, the galaxy also lies in the quiescent wedge of the rest-frame *(U-V)* vs. *(V-J)* (*UVJ*) color-color diagram, consistent with the positions of post-starburst galaxies.

2.2. *Spectroscopic Follow-up*

We obtained deep spectra of XMM-2599 using the MOSFIRE spectrograph (McLean et al. 2010, 2012) on the Keck I telescope (PI Wilson; Figure 2). Observations were taken in November and December of 2018. A single mask was observed in K-band for $2^{\rm h}45^{\rm m}$, with an average seeing of $0.6''$, as determined from a slit star. Two masks in H-band were observed for on-source times of $2^{\rm h}20^{\rm m}$ and $2^{\rm h}40^{\rm m}$, with seeing of $0.94''$ and $1.13''$, respectively.

SED

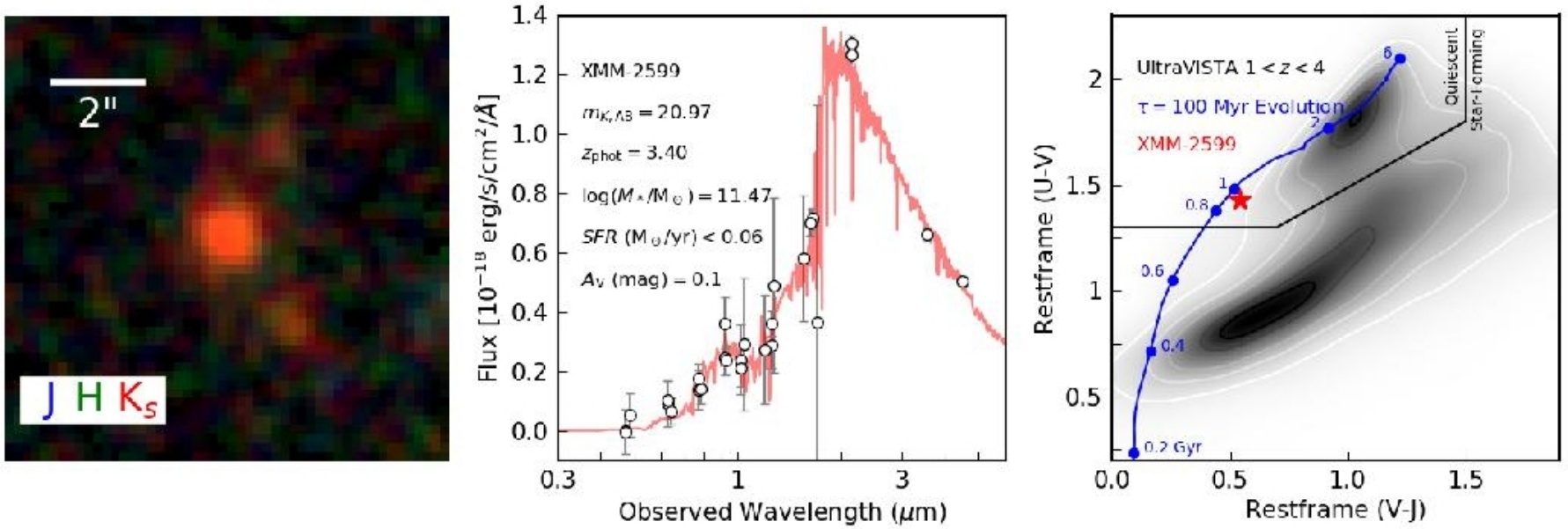

Figure 1. Photometric properties of XMM-2599. **Left:** Near-infrared imaging of XMM-2599. **Middle:** Photometric spectral energy distribution of XMM-2599. Data are shown in white with gray 1σ errorbars, while the best fit template to the photometry alone is shown in red. Listed properties are also derived from the photometry alone. **Right:** XMM-2599 on the restframe UVJ diagram. A mass-complete sample of galaxies at $1 < z < 4$ from UltraVISTA are shown in gray for comparison. The evolution of a population with an exponentially-declining star-formation history parameterized by $\tau = 100$ Myr is shown in blue, with several ages labeled in Gyr.

Спектр

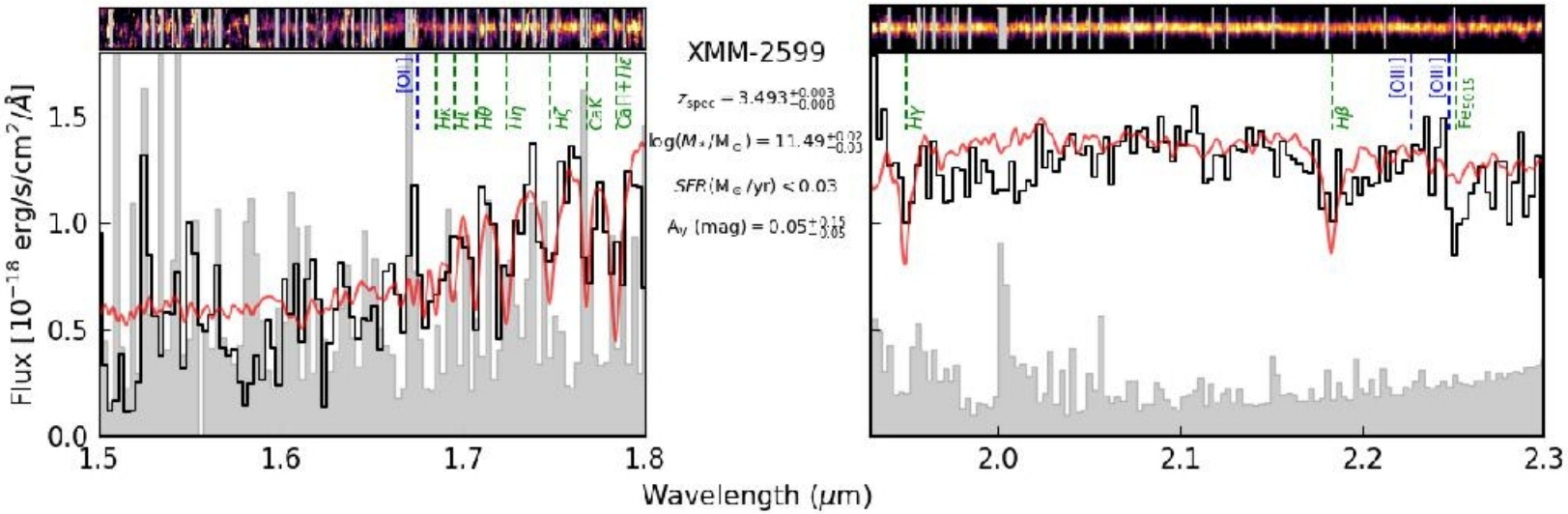

Figure 2. Near-infrared H and K band spectra for XMM-2599 and best-fit model. **Top:** The telluric corrected 2D spectra, smoothed for visual clarity. Strong sky lines are masked with gray lines. **Bottom:** The 1D extracted spectra, shown in bins 30 Å wide, are black, while the 1σ noise (including telluric correction) is gray. The best fit template to the combined photometry and spectroscopy is plotted in red. The location of absorption features are indicated in green, and the wavelengths corresponding to nebular emission from oxygen are blue.

История звездообразования

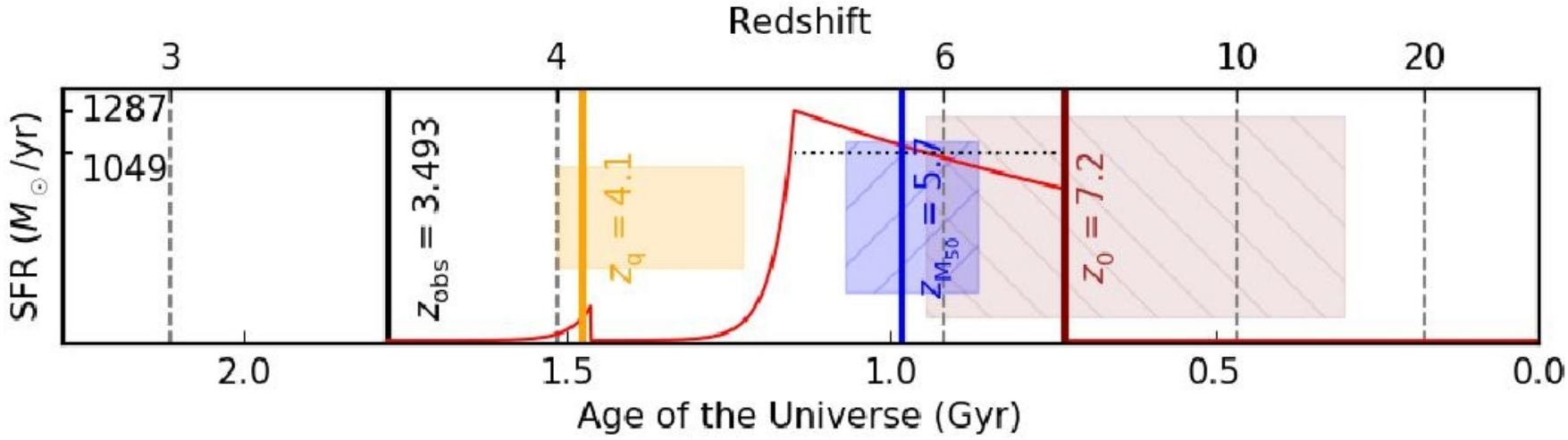

Figure 3. Best fit star-formation history for XMM-2599. The red curve indicates the SFR over cosmic time, with the maximum SFR and a characteristic average SFR shown in solar masses per year on the y-axis. The black line indicates the spectroscopic redshift and the maroon line is the time that the galaxy began forming stars. The orange line is the time at which SFR drops below 10% of the previous average SFR while the blue line denotes the time at which half of the final stellar mass has been formed. Shaded regions correspond to 1σ confidence intervals.

Сравнение с наимоднейшей LCMD-симуляцией: мимо!

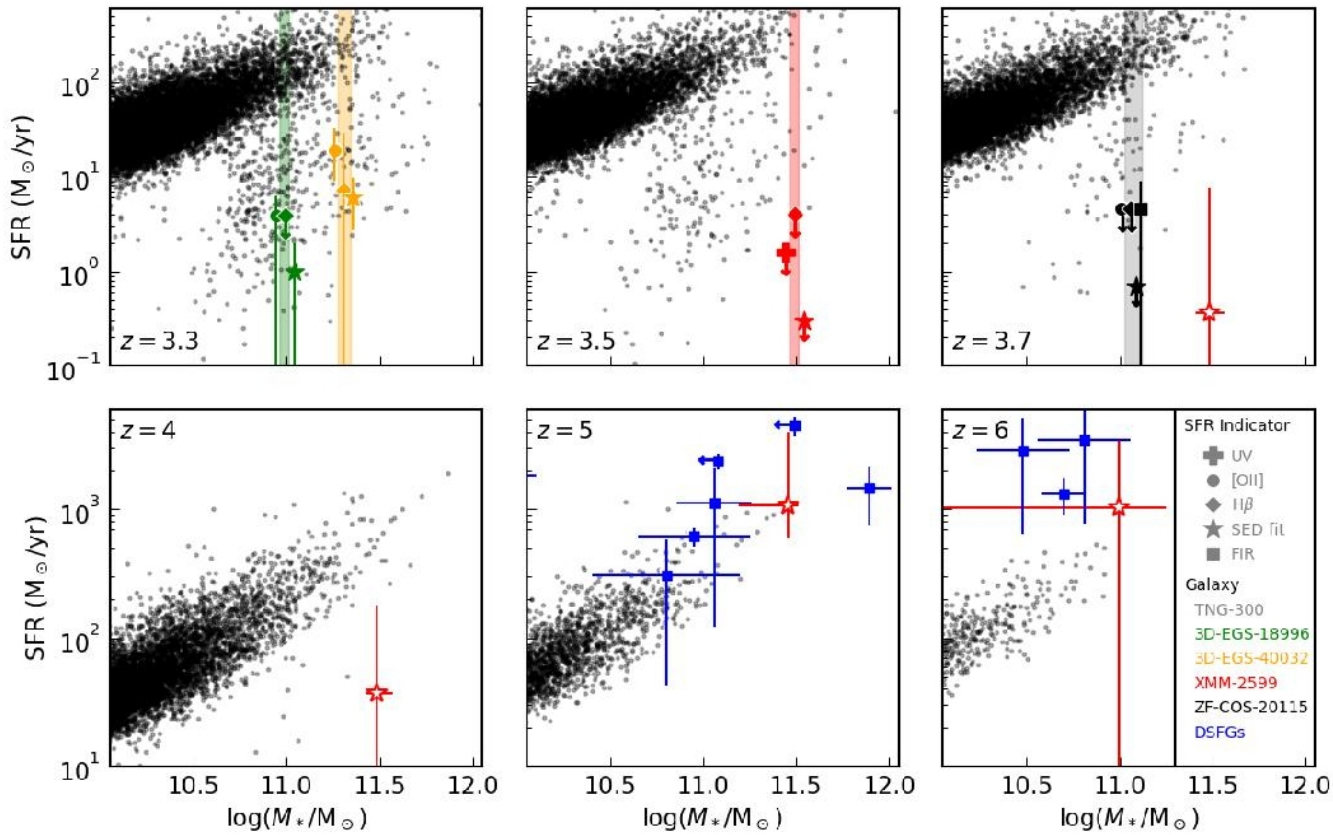

Figure 5. Comparison to the Illustris TNG-300 simulation on the SFR-M_* plane. We show the spectroscopically confirmed absorption-line identified UMGs at $z_{\rm spec} > 3$ (green, orange, red, and black), simulated galaxies from six snapshots in Illustris TNG-300 (gray), and the DSFGs from Figure 4 (blue). Several probes of star formation are shown differentiated by marker